Squirrel-cage induction motor parameter determination using instantaneous power

Hengameh Kojooyan-Jafari, Lluis Monjo, *Student Member, IEEE,* Felipe Córcoles, Joaquin Pedra, *Member, IEEE*

Abstract—A new parameter determination method for squirrel-cage induction motors is presented. It is based on the double-cage model and uses experimental data from starting transient measurements. The double-cage model parameters are estimated with the values of the equivalent impedances calculated at several points (1) between the maximum torque point and synchronism from a single-cage model and (2) at speed points where the double-cage effect is significant from the measured stator instantaneous power. Three motors were tested in the laboratory and the proposed method was applied to obtain their parameters. The steady-state torque- and current-slip curves predicted by the estimated parameters are compared with those measured in the laboratory to check the accuracy of the method.

***Index Terms*—Parameter estimation, double-cage model, starting transient measurements.**

I. Introduction

THE accuracy of motor parameters in simulations is crucial in performance prediction of electric power disturbance, motor starting or advanced control techniques. IEEE Std-112 [1] and IEC Rotating electrical machines-Part 28 [2] describe the most usual parameter estimation methods, which are based on short-circuit and no-load tests. An important review of induction motor estimation techniques can be found in [3].

The main parameter estimation techniques from experimental measurements are based on

- Steady-state measurements [1],[2],[4],[5]
- Variable frequency measurements [6]-[9]
- Transient measurements [10]-[22]

The simplest and most common parameter estimation procedures are based on steady-state measurements. Ref. [7] gives a brief introduction to these techniques based on dc, no-load and short-circuit tests. Moreover, two Standards for this kind of procedures have been published, [1][2]. Finally, advances in steady-state parameter estimation via linear regression can be found in [4].

Methods based on variable frequency tests can be divided into two types: those using sources with tunable voltage and frequency [6][7] and those using sources with PWM voltage waveform [8][9].

This research work has been supported by grant ENE2009-10274.

Hengameh Kojooyan-Jafari, Ll. Monjo, F. Córcoles and J. Pedra are with the Department of Electrical Engineering, ETSEIB-UPC, Av. Diagonal 647, 08028 Barcelona, Spain (e-mail: kojooyan@iiau.ac.ir, lluis.monjo@upc.edu, corcoles@ee.upc.es, pedra@ee.upc.es)

Finally, methods based on transient measurements can be classified in three categories:

- Kalman filter methods [10]-[12]
- Linear least square methods [13]-[17]
- Non-linear least square methods [18]-[22]

The extended Kalman filter is an algorithm for optimal state estimation of non-linear systems in the presence of noise [10]-[12].

Linear least square methods manipulate electric machine differential equations to eliminate the non-measurable magnitudes of the rotor (rotor currents or fluxes) [13]-[16]. This paper applies a new method that uses an approximation of the rotor flux to improve the accuracy of the estimation procedure [17].

In non-linear least square methods, an error function is calculated with measured and simulated currents. These techniques have a high computational cost because each evaluation of the error function requires a transient simulation. The use of this error function in a minimization algorithm defines a parameter estimation method with different approaches [18]-[21].

Other methodologies using instantaneous rms current measurements as steady-state values are presented in [22] and [23].

All these methodologies are largely applied to parameter estimation of the induction machine with single-cage model (Fig. 1a). This model can be adequate for wound rotor motors or some small motors. The double-cage model (Fig. 1b) is usually necessary to justify the experimental starting torque and current measurements in small, medium and large motors (Fig.2b) [24][25].

Double-cage model parameter estimation has been studied using steady-state data only. There are no references in the literature using both the double-cage model and transient measurements. The minimum number of parameters that characterize the double-cage model is studied in [26] whereas parameter estimation procedures based on steady-state data are presented in [27] and [28]. A Matlab/Simulink function “Power_Asynchronous Machine Params” is based on the above works [29]. Finally, [30] mentions the double-cage model parameter estimation problem, but does not provide a clear methodology to perform the estimation.

The main objective of this paper is to present a new method for parameter estimation using the double-cage model based on instantaneous voltages, currents and speed measured in a free-acceleration test.

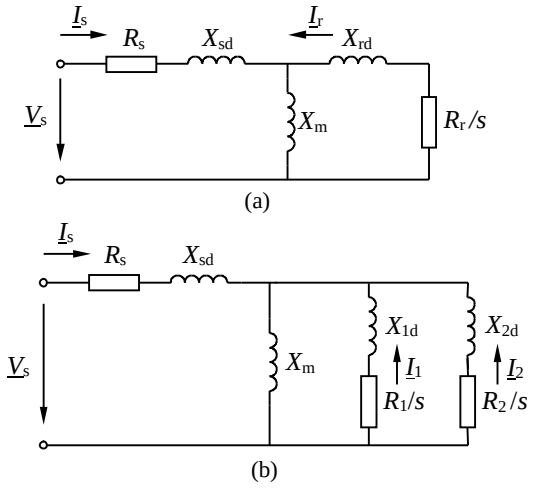

Fig. 1. Steady-state star equivalent circuit for the (a) single-cage and (b) double-cage models of the squirrel-cage induction motor.

II. Induction Motor Model

A. Steady-state modeling

The circles in Fig. 2 represent the steady-state torque and current of two medium-sized ABB motors measured by the manufacturer (catalogue data are summarized in Table I). Table II contains the single- and double-cage model parameters estimated from these measurements. The curves predicted by both models are also plotted in Fig. 3. As expected, the double-cage model (solid line) exhibits good agreement between measurements and predictions whereas the single-cage model (dotted line) only provides accurate results between the maximum torque point and synchronous speed. Fig. 3 shows

TABLE I
CATALOGUE DATA OF TESTED SQUIRREL-CAGE INDUCTION MOTORS

Motor	P_N (kW)	U_N (V)	f_N (Hz)	PF_N	ω_N (r/min)	η_N (%)	T_{MAX}/T_N	T_{ST}/T_N	I_{ST}/I_N	J (kg·m^2)
#1	75	400	50	0.86	1480	93.6	4.7	3.8	5.9	4.9
#2	37	400	50	0.83	985	92.3	4.0	4.6	5.8	3.1
#3	1.5	400	50	0.69	940	79.1	2.3	1.7	3.9	0.115*
#4	2.2	400	50	0.80	1430	86.0	2.6	2.3	6.3	0.200*
#5	2.2	400	50	0.75	950	86.7	3.4	3.1	7.1	0.193*

* These values include the inertia of the DC machine connected to the shaft of the machine.

clearly that the squirrel-cage motor must be represented with the double-cage model [25][26]. This figure also contains the values predicted from the parameters estimated by the proposed method (dashed line).

B. Transient modeling

The dynamic equations of the single-cage induction motor model in synchronous reference frame are

$$\begin{aligned} v_s &= \left(R_s + L_s\left(p + \mathrm{j}\omega\right)\right)i_s + M\left(p + \mathrm{j}\omega\right)i_r \\ 0 &= M\left(p + \mathrm{j}s\omega\right)i_s + \left(R_r + L_r\left(p + \mathrm{j}s\omega\right)\right)i_r \\ T(t) &= 2\wp M\,\mathrm{Im}\left(i_s i_r^*\right) \quad , \quad s = \left(\omega - \wp\omega_m\right)/\omega. \end{aligned} \tag{1}$$

where $\wp$ is the number of pairs of poles, ω is the synchronous speed, ω_m is the mechanical speed, s is the slip and the parameters are

$$M = X_m/\omega \quad ; \quad L_s = \left(X_{sd} + X_m\right)/\omega \quad ; \quad L_r = \left(X_{rd} + X_m\right)/\omega \tag{2}$$

The dynamic equations of the double-cage induction motor

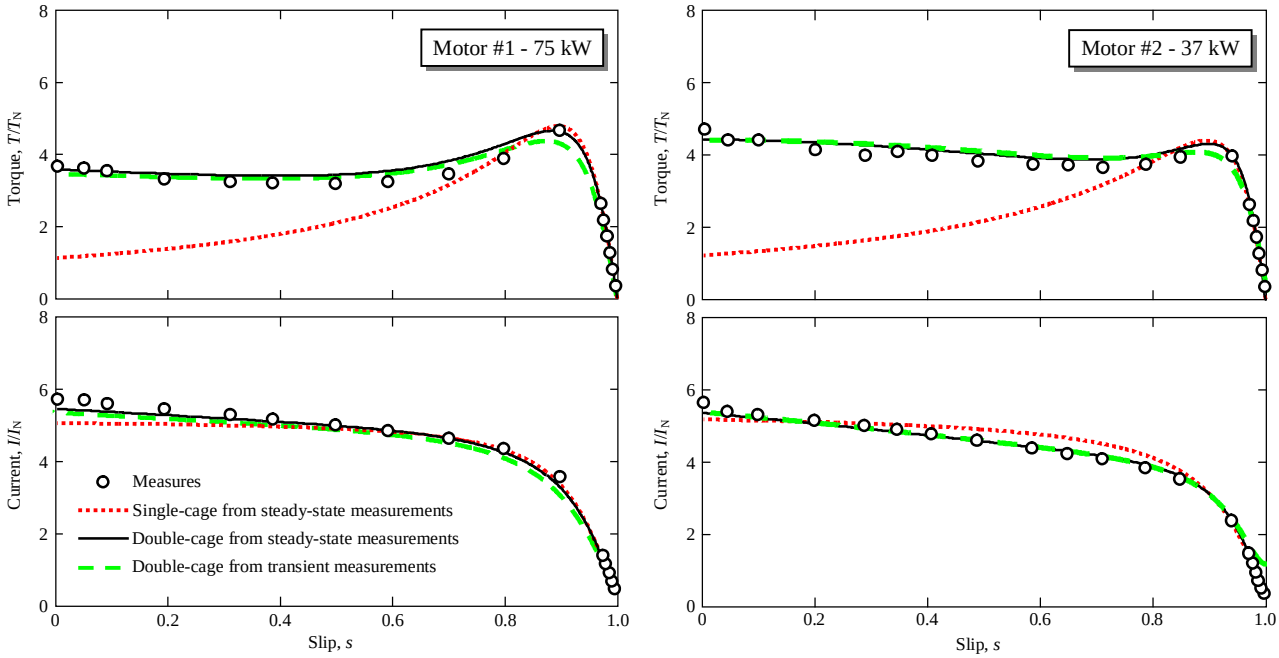

Fig. 2. Measured (marked with points) and predicted torque- and current-slip curves for motors #1 and #2. Models used for torque and current prediction: Single-cage model from steady-state measurements (dotted line), double-cage model from steady-state measurements (solid line) and double-cage model from transient measurements (discontinuous line).

TABLE II
ESTIMATED PARAMETERS FOR THE SINGLE- AND DOUBLE-CAGE MODELS IN PU ($S_B = P_N$, $U_B = U_N$, $Z_B = U_B^2/S_B$)

	Single-cage model				Double-cage model					
	r_s	$x_{sd} = x_{rd}$	x_m	r_r	r_s	$x_{sd} = x_{2d}$	x_m	r_1	x_{1d}	r_2
Motor #1	0.0280	0.0810	1.5156	0.0169	0.0544	0.0474	1.9051	0.0182	0.1108	0.1964
Motor #2	0.0716	0.0633	2.1839	0.0150	0.0647	0.0379	1.9587	0.0166	0.1416	0.1092

model in synchronous reference frame are

$$\begin{aligned} v_s &= \left(R_s + L_s\left(p + \mathrm{j}\omega\right)\right)i_s + M\left(p + \mathrm{j}\omega\right)i_1 + M\left(p + \mathrm{j}\omega\right)i_2 \\ 0 &= M\left(p + \mathrm{j}s\omega\right)i_s + \left(R_1 + L_1\left(p + \mathrm{j}s\omega\right)\right)i_1 + M\left(p + \mathrm{j}s\omega\right)i_2 \\ 0 &= M\left(p + \mathrm{j}s\omega\right)i_s + M\left(p + \mathrm{j}s\omega\right)i_1 + \left(R_2 + L_2\left(p + \mathrm{j}s\omega\right)\right)i_2 \\ T\left(t\right) &= 2.\wp.M.\mathrm{Im}\left(i_s\left(i_1^* + i_2^*\right)\right) \quad , \quad s = \left(\omega - \wp\,\omega_m\right)/\omega, \end{aligned} \tag{3}$$

where the parameters are

$$\begin{aligned} M = X_m/\omega \quad ; \quad L_s = \left(X_{sd} + X_m\right)/\omega \\ L_1 = \left(X_{1d} + X_m\right)/\omega \quad ; \quad L_2 = \left(X_{2d} + X_m\right)/\omega. \end{aligned} \tag{4}$$

The relation between the Ku variables (complex) and the Park variables is

$$x_s = \frac{x_{sd} + \mathrm{j}x_{sq}}{\sqrt{2}} \quad ; \quad x = v, i \tag{5}$$

The instantaneous stator currents and voltages can be transformed into Park variables according to the following equation:

$$\begin{aligned} x_{sd} &= \sqrt{\frac{2}{3}}\left\{x_{sa}\cos\theta + x_{sb}\cos\left(\theta - \frac{2\pi}{3}\right) + x_{sc}\cos\left(\theta + \frac{2\pi}{3}\right)\right\} \\ x_{sq} &= -\sqrt{\frac{2}{3}}\left\{x_{sa}\sin\theta + x_{sb}\sin\left(\theta - \frac{2\pi}{3}\right) + x_{sc}\sin\left(\theta + \frac{2\pi}{3}\right)\right\} \\ x &= v, i \end{aligned} \tag{6}$$

where θ is the Park's transformation angle.

Fig. 3 shows the simulated torque, direct and quadrature currents, and the mechanical speed obtained from the simulation of a free-acceleration starting test on motors #1 and #2 using the double-cage model obtained from the catalogue data with the parameters in Table I. The simulation was made at rated voltage (U = 400V) and with the catalogue inertia (Table I). The values of dq currents and speed in Fig. 3, together with the dq voltages, are the data for the estimation parameter method proposed in the paper.

The main limitation in squirrel-cage induction motor parameter determination is non-measurable rotor currents. The single-cage model allows equations to be rewritten without using the rotor magnitudes [13]-[17]. No similar deduction

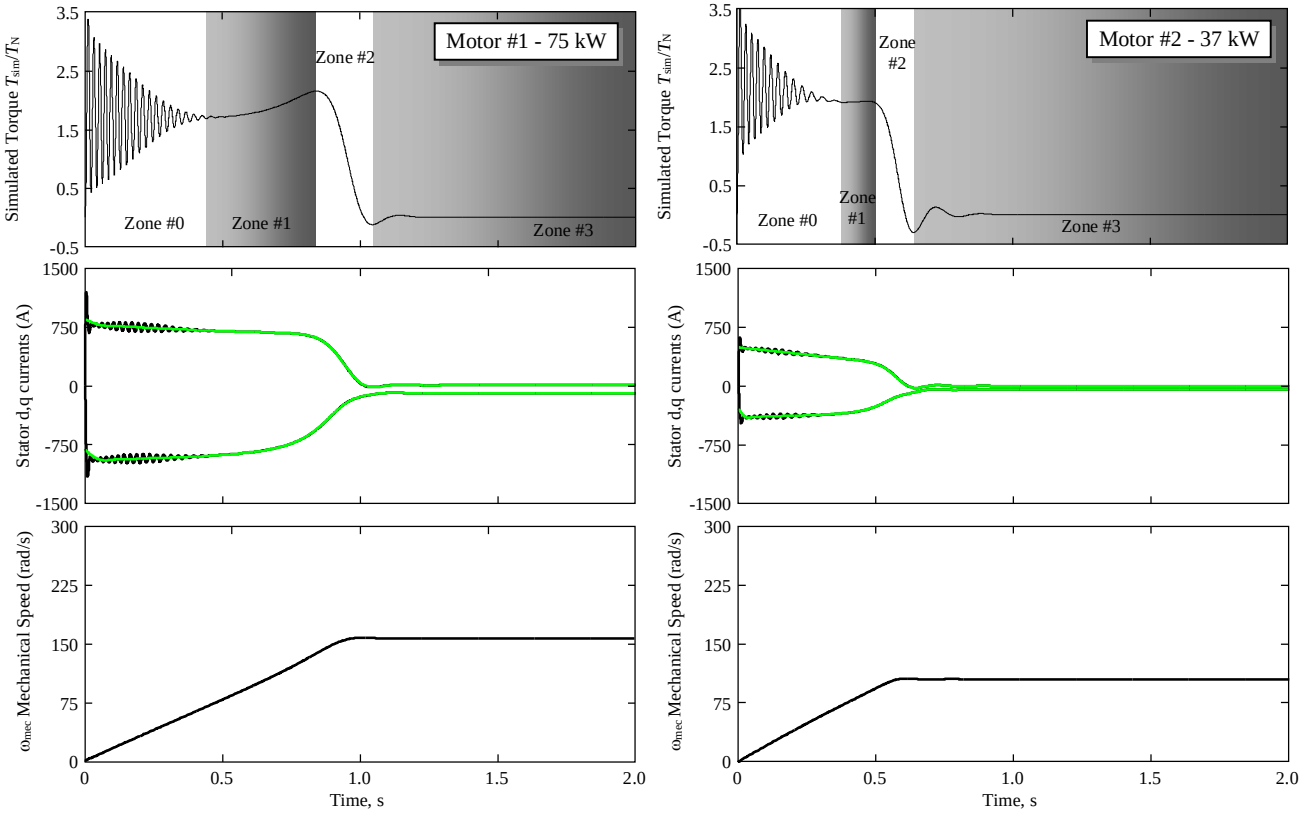

Fig. 3. Simulated torque, direct and quadrature currents, and mechanical speed in a free-acceleration starting test on motors #1 and #2.

for the double-cage model has been found in the literature.

III. Proposed Method

A. Description and justification

The proposed estimation method fits the machine impedances ($\underline{Z}_{meas}$) during a free-acceleration test. The selection of impedances can be justified with the help of simulation in Fig. 3. This figure shows the simulated dynamic electromagnetic torque, transformed currents and mechanical speed during a free-acceleration test. As can be seen, Fig. 3a contains different data zones that will be used in the proposed method.

The estimation procedure is composed of the following two steps. The first uses the data in zones #2 and #3 because, as observed in Fig. 2, the torque predicted for the single- and double-cage models exhibits good agreement with that measured between the maximum torque point and the synchronous speed point. This fact is exploited to fit the parameters of a single-cage model with the data in zones #2 and #3 (Section III.B) using the algorithm described in [17] and repeated here for clarity. The second step, the instantaneous power method, uses data in zones #0 and #1 (Section III.C) to fit the parameters of a double-cage model in order to exploit the dominant double-cage effect in Fig. 2.

B. Estimation of a Single Cage

In [17] it is justified that the elimination of the non-measurable rotor currents in (1) leads to the following set of linear equations:

$$\begin{pmatrix} a_{d1} & a_{d2} & a_{d3} & a_{d4} & a_{d5} & a_{d6} \\ a_{q1} & a_{q2} & a_{q3} & a_{q4} & a_{q5} & a_{q6} \end{pmatrix} \begin{pmatrix} K_1 \\ K_2 \\ K_{31} \\ K_{32} \\ K_4 \\ K_5 \end{pmatrix} = \begin{pmatrix} b_d \\ b_q \end{pmatrix} \tag{7}$$

where

$$\begin{aligned} &a_{d1} = \frac{di_{sd}}{dt};\ a_{d2} = i_{sd};\ a_{d3} = -\left(\omega - \wp\,\omega_{mec}\right) i_{sq};\ a_{d4} = -\omega i_{sq} \\ &a_{d5} = -\left(\frac{dv_{sd}}{dt} - \left(\omega - \wp\,\omega_{mec}\right) v_{sq} + \frac{1}{\omega}\frac{d\,\wp\,\omega_{mec}}{dt} v_{sd} \right);\ a_{d6} = -v_{sd} \end{aligned} \tag{8}$$

$$\begin{aligned} b_d = &-\frac{d^2 i_{sd}}{dt^2} + \left(2\omega - \wp\,\omega_{mec}\right)\frac{di_{sq}}{dt} + \\ &+ \omega\left(\omega - \wp\,\omega_{mec}\right) i_{sd} - \frac{d\,\wp\,\omega_{mec}}{dt} i_{sq} \end{aligned} \tag{9}$$

$$\begin{aligned} &a_{q1} = \frac{di_{sq}}{dt};\ a_{q2} = i_{sq};\ a_{q3} = \left(\omega - \wp\,\omega_{mec}\right) i_{sd};\ a_{q4} = \omega i_{sd} \\ &a_{q5} = -\left(\frac{dv_{sq}}{dt} + \left(\omega - \wp\,\omega_{mec}\right) v_{sd} - \frac{1}{\omega}\frac{d\,\wp\,\omega_{mec}}{dt} v_{sq} \right);\ a_{q6} = -v_{sq} \end{aligned} \tag{10}$$

$$\begin{aligned} b_q = &-\frac{d^2 i_{sq}}{dt^2} - \left(2\omega - \wp\,\omega_{mec}\right)\frac{di_{sd}}{dt} + \\ &+ \omega\left(\omega - \wp\,\omega_{mec}\right) i_{sq} + \frac{d\,\wp\,\omega_{mec}}{dt} i_{sd} \end{aligned} \tag{11}$$

Use of *n* data points leads to the following overdetermined linear system:

$$\begin{pmatrix} a_{d1}^1 & a_{d2}^1 & a_{d3}^1 & a_{d4}^1 & a_{d5}^1 & a_{d6}^1 \\ a_{q1}^1 & a_{q2}^1 & a_{q3}^1 & a_{q4}^1 & a_{q5}^1 & a_{q6}^1 \\ a_{d1}^2 & a_{d2}^2 & a_{d3}^2 & a_{d4}^2 & a_{d5}^2 & a_{d6}^2 \\ a_{q1}^2 & a_{q2}^2 & a_{q3}^2 & a_{q4}^2 & a_{q5}^2 & a_{q6}^2 \\ \vdots & \vdots & \vdots & \vdots & \vdots & \vdots \\ a_{d1}^n & a_{d2}^n & a_{d3}^n & a_{d4}^n & a_{d5}^n & a_{d6}^n \\ a_{q1}^n & a_{q2}^n & a_{q3}^n & a_{q4}^n & a_{q5}^n & a_{q6}^n \end{pmatrix} \begin{pmatrix} K_1 \\ K_2 \\ K_{31} \\ K_{32} \\ K_4 \\ K_5 \end{pmatrix} = \begin{pmatrix} b_d^1 \\ b_q^1 \\ b_d^2 \\ b_q^2 \\ \vdots \\ b_d^n \\ b_q^n \end{pmatrix} \tag{12}$$

which can be rewritten as

$$\mathbf{Ax = b} \tag{13}$$

This overdetermined linear system is solved by the least square regression method,

$$\mathbf{x} = \left(\mathbf{A}^t\mathbf{A}\right)^{-1}\mathbf{A}^t\mathbf{b} \tag{14}$$

where $\mathbf{x} = (K_1, K_2, K_{31}, K_{32}, K_4, K_5)$.

The estimated parameters are (K_1, K_2, K_{31}, K_{32}, K_4, K_5). The induction motor electrical parameters can be calculated from the above parameters considering the following restriction $L_{sd} = L_{rd}$ [26]:

$$\begin{aligned} &L_s = L_r = \frac{K_5}{K_{32}} \quad ; \quad \sigma = \frac{1}{K_4 L_s} \quad ; \quad M = \sqrt{(1-\sigma) L_s^2} \\ &R_s = \frac{L_s}{T_s} = L_s \sigma K_{31} \quad ; \quad R_r = \frac{L_r}{T_r} = L_r \sigma K_{32} \\ &L_{sd} = L_{rd} = L_s - M \end{aligned} \tag{15}$$

By using the single-cage model estimated parameters $\left(R_s, R_r, X_{sd}, X_{rd}, X_m\right)$, impedance values at speeds in the range between the maximum torque point and synchronous speed are determined by

$$\underline{Z}_k\left(s_k\right) = R_s + jX_{sd} + \frac{1}{\dfrac{1}{jX_m} + \dfrac{1}{R_r/s_k + jX_{rd}}}. \tag{16}$$

C. Instantaneous Power Method

The active and reactive power can be calculated for any measured instant from the experimental data (voltages and currents):

$$P(t) = \frac{1}{T}\int_{t-T/2}^{t+T/2} p(t)\,dt = \frac{1}{T}\int_{t-T/2}^{t+T/2} \left(v_a \cdot i_a + v_b \cdot i_b + v_c \cdot i_c\right) dt \tag{17}$$

$$I(t)=\sqrt{\frac{1}{T}\int_{t-T/2}^{t+T/2}\frac{\left(i_a^2+i_b^2+i_c^2\right)}{3}\mathrm{d}t} \tag{18}$$

$$U(t)=\sqrt{\frac{1}{T}\int_{t-T/2}^{t+T/2}\frac{\left(u_a^2+u_b^2+u_c^2\right)}{3}\mathrm{d}t} \tag{19}$$

$$S(t)=3U(t)\cdot I(t) \tag{20}$$

$$Q(t)=\sqrt{S(t)^2-P(t)^2} \tag{21}$$

By choosing specific slip points $s_k = s(t_k)$, it is possible to determine the impedance at such slips:

$$\underline{Z}_k\left(s(t_k)\right)=\frac{3U_k^2}{P\left(s(t_k)\right)-\mathrm{j}Q\left(s(t_k)\right)}. \tag{22}$$

Next, we will focus on the validity of the approximated expressions for the instantaneous active and reactive power in (17) and (21).

An approximation of the torque can be calculated using the equation

$$\Gamma_e(t)\approx\frac{P(t)-3R_sI^2(t)}{\left(\omega_s/\wp\right)} \tag{23}$$

Fig. 4a compares the approximated dynamic torque calculated with (23) and the exact dynamic torque calculated with (3). Excellent matching between both torques is observed when the dynamic torque oscillations vanish.

Fig. 4b illustrates the approximated dynamic torque in (23) and the steady-state torque curves, where the axis is now the slip. Note the good agreement between the torques in the zone between the maximum torque point and the end of the electromagnetic transient. Moreover, if the estimated torque is smoothed [19], it agrees well with the steady-state torque, which lies in the zone between the maximum torque point and near-zero speed (Fig. 4c).

Fig. 4 shows that the maximum steady-state torque is always greater than the maximum torque obtained in a transient process. This phenomenon is pointed out in [4].

The agreement between the smoothed estimated torque and the steady-state torque lead us to conclude that, the impedance values calculated by the instantaneous power method can be a good approximation of the double-cage parameters in the zone between the maximum torque point and zero speed.

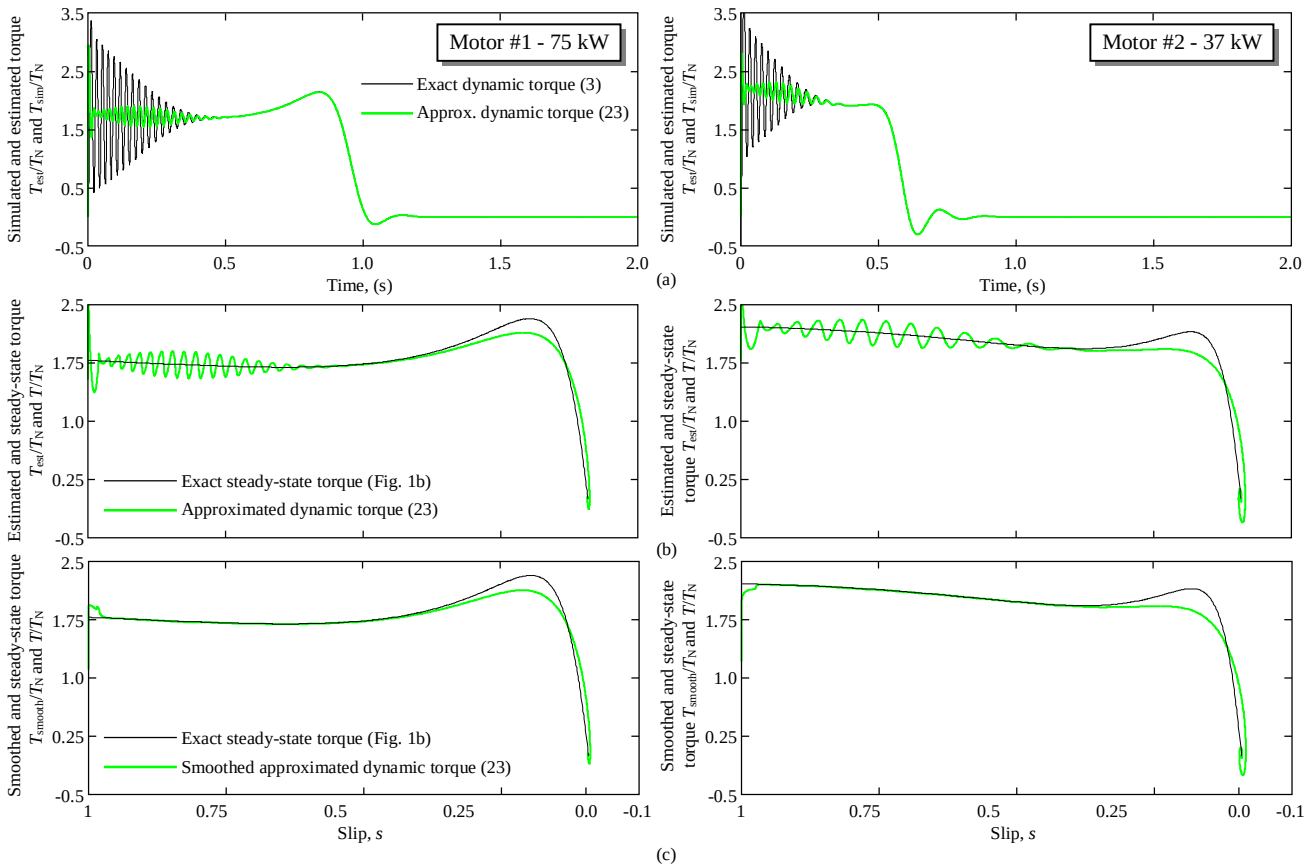

Fig. 4. (a) Simulated and estimated instantaneous torque, (b) simulated steady-state torque and estimated instantaneous torque and (c) simulated steady-state torque and smoothed estimated instantaneous torque for motors #1 and #2

TABLE III
ESTIMATED PARAMETERS FOR THE DOUBLE-CAGE MODEL IN PU
($S_B = P_N$, $U_B = U_N$, $Z_B = U_B^2/S_B$)

	r_s	$x_{sd} = x_{2d}$	x_m	r_1	x_{1d}	r_2
Motor #1	0.0548	0.0501	1.5011	0.0183	0.1119	0.1788
Motor #2	0.0647	0.0394	1.6997	0.0161	0.1449	0.1030
Motor #3	0.0363	0.0696	1.0781	0.0331	0.0812	0.2874
Motor #4	0.0268	0.0562	1.1500	0.0254	0.0738	0.1698
Motor #5	0.0359	0.0861	1.0202	0.0314	0.1149	0.1701

D. Double-cage Parameter Determination

As explained above, the method proposed for double-cage model parameter estimation from the free-acceleration starting test uses two sets of measured impedances:

- The first set of machine impedances is obtained from a single-cage model previously estimated with data in the range between the maximum torque point and steady-state speed.
- The second set of machine impedances is calculated by the instantaneous power method, using data in the range between the maximum torque point and zero speed.

E. Least Square Algorithm for Parameter Estimation

The double-cage model has six unknown parameters $(R_s, R_{r1}, R_{r2}, X_{sd}, X_{1d}, X_{2d}, X_m)$, where $X_{sd} = X_{2d}$ [26]. The impedance at the slip point s_n corresponding to the speed $\omega_{mec\,n}$ is

$$\underline{Z} = R_s + jX_{sd} + \frac{1}{\frac{1}{jX_m} + \frac{1}{R_1/s_n + jX_{1d}} + \frac{1}{R_2/s_n + jX_{2d}}}, \quad (24)$$

The impedance of the double-cage model is defined using the analytical expressions of (24):

$$\underline{Z}(\omega_{mec\,n}) = R(\mathbf{x}, \omega_{mec\,n}) + jX(\mathbf{x}, \omega_{mec\,n}) \quad (25)$$

where $\mathbf{x} = (R_s, R_1, R_2, X_{sd}, X_m, X_{1d})$. The error functions are defined as

$$\varepsilon_{Rn} = \frac{R_{meas}(s_k) - R_{calc}(\mathbf{x}, s_k)}{R_{tran}(\omega_{mec\,n})}$$
$$\varepsilon_{Xn} = \frac{X_{meas}(s_k) - X_{calc}(\mathbf{x}, s_k)}{X_{meas}(s_k)} \quad (26)$$

Finally, the parameters are estimated by solving the minimization problem

$$\min\{F(\mathbf{x})\} = \min\left\{\sum_{n=1}^{N} w_n \left(\varepsilon_{Rn}^2(\mathbf{x}, s_k) + \varepsilon_{Xn}^2(\mathbf{x}, s_k)\right)\right\} \quad (27)$$

where N is the number of points and w_n is a value to assign a weight to the points used in the single-cage model (Section II). In this paper all weights are 1.

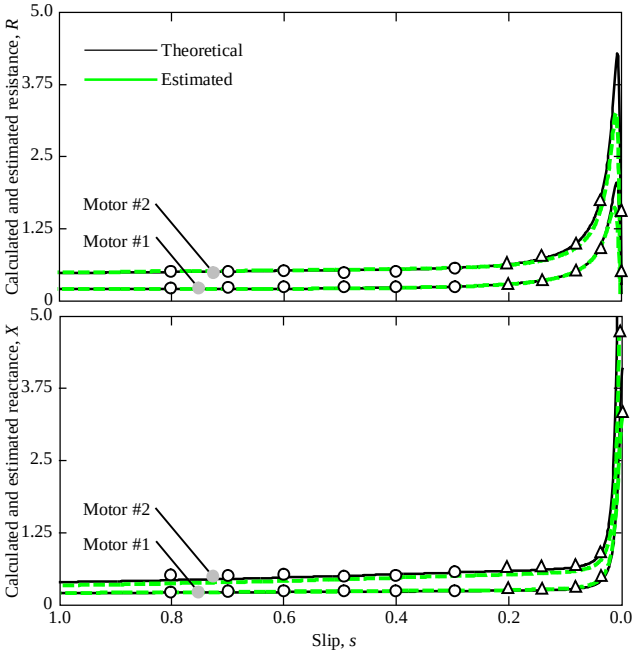

Fig. 5. Simulation of the real and calculated resistance- and reactance-slip for #motor 1 and #motor 2

The parameters are estimated by the Matlab function `lsqnonlin` [31].

F. Estimation Results Analysis

Table III contains the parameters estimated using the free-acceleration starting test on motors #1 and #2. Fig. 2 shows the torque- and current-speed curves predicted with these parameters (dashed lines). It can be observed that the results predicted by the proposed method show good agreement with the manufacturer data.

Fig. 5 shows the values calculated with the single-cage model (triangles) (Section IV) and the resistance and reactance values calculated by the instantaneous power method (circles) (Section V). The resistance and reactance values calculated with the double-cage model in Fig. 1b using the parameters of Table II are also given (solid line), as well as the values calculated with the parameters obtained by the proposed method (Table III) (dotted line).

IV. EXPERIMENTAL VALIDATION

To validate the proposed method, motors #3, #4 and #5 in Table I were tested in the laboratory. A free-acceleration starting test at a reduced voltage was performed on each motor to estimate the double-cage model parameters. Steady-state torque- and current-slip measurements were made at different speeds for performance comparison.

Each motor was tested at the voltage that makes its nominal current flow at zero speed to avoid leakage reactance saturation. In this way, a similar saturation effect was obtained in steady-state and transient conditions. The voltage used in the tests is $0.52U_N$ for motor #1, $0.24U_N$ for motor #2 and $0.28U_N$ for motor #3. To make the tests comparable, the torque and

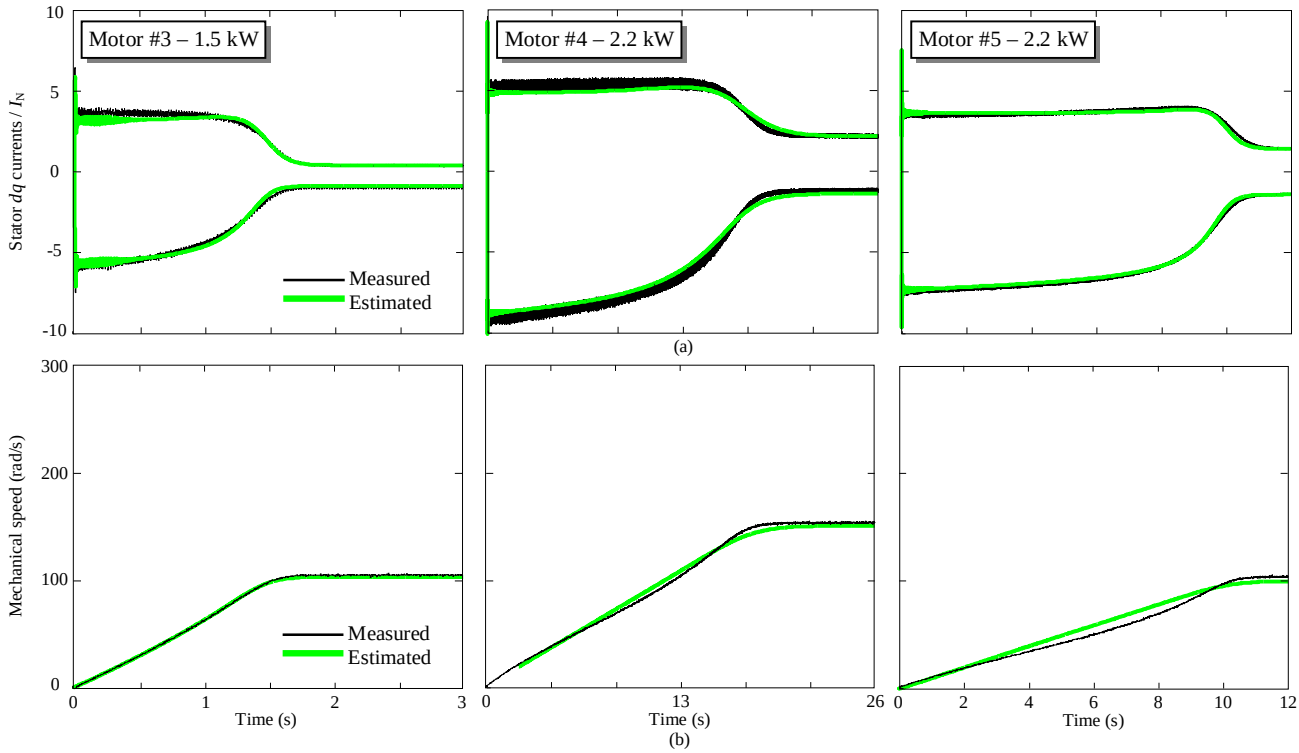

Fig. 6. (a) Measured and estimated direct and quadrature stator current and (b) mechanical speed in a free acceleration test.

current were prorated to rated values:

$$T_{\text{prorated}} = T_{\text{measured}} \left(\frac{U_{\text{N}}}{U} \right)^2 \quad ; \quad I_{\text{prorated}} = I_{\text{measured}} \left(\frac{U_{\text{N}}}{U} \right) \tag{28}$$

where U_{N} is the nominal value.

Fig. 6 shows the Park currents and the mechanical speed measured in the free-acceleration starting test. These measurements were used to calculate the parameters of the double-cage model in Table III.

Fig. 7 compares the estimated torque- and current-slip curves calculated with the parameters in Table III (solid lines) with the steady-state torque and current measurements (circles). As can be seen, the agreement between the predicted and measured torque and current curves in the three motors is excellent.

V. Conclusions

This paper presents a new parameter estimation method for the double-cage model of squirrel-cage induction machine which uses measurements of stator voltages, currents and mechanical speed in a free-acceleration starting transient.

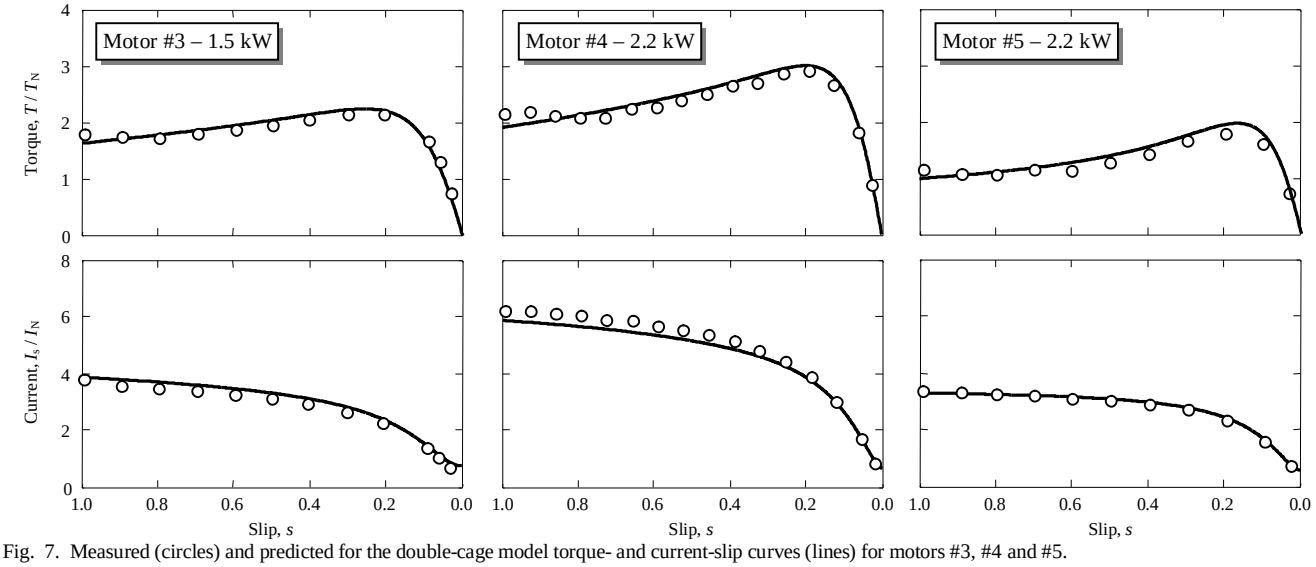

Fig. 7. Measured (circles) and predicted for the double-cage model torque- and current-slip curves (lines) for motors #3, #4 and #5.

The method calculates the values of the equivalent impedance at different speeds which are subsequently processed by the least square method to obtain the parameters of the double-cage model. The impedances are calculated from: (1) the data measured from the maximum torque point to steady-state speed and estimating the parameters of a single-cage model, and (2) the data in the zone where the double-cage effect is significant (between the maximum torque point and zero speed) and using the instantaneous power method.

The method was tested on three motors in the laboratory for validation. The torque- and current-slip curves predicted with the estimated parameters and the curves measured in the laboratory show excellent agreement.

VI. Acknowledgments

The authors would like to thank Amalia Barrera and Francesc Quintana from Asea Brown Boveri, S. A., Fábrica de Motores, for providing the experimental data of the motors in Fig. 2.

VII. References

[1] IEEE Standard test procedure for polyphase induction motors and generators, IEEE Std. 112-2004, Nov. 2004.

[2] IEC Rotating electrical machines-Part 28: Test methods for determining quantities of equivalent circuit diagrams for three-phase low-voltage cage induction motors, IEC 60034-28 Ed. 2.0 (2012-12)

[3] H. A. Toliyat, E. Levi, M. Raina, "A review of RFO induction parameter estimation techniques", IEEE Trans. Energy Conversion, Vol. 18, No.2, June 2003, pp. 271-283.

[4] E. Laroche, M. Boutayeb, "Identification of the induction motor in sinusoidal mode", IEEE Trans. Energy Conversion, Vol. 25, No.1, March 2010, pp. 11-19.

[5] S. Ayasun, C. O. Nwankpa, "Induction motor test using MATLAB/Simulink and their integration into undergraduate electric machinery courses", IEEE Trans. Education, Vol. 48, No.1, Feb. 2005, pp. 37-46.

[6] I. Zubia, A. Zatarain, C. Alcalde, X. Ostolaza, "In situ electrical identification meted for induction wind generators", IET Electric Power Applications, Vol. 5, No. 7, 2011, pp. 549-557.

[7] M. O. Sonnaillon, G. Bisheimer, C. De Angelo, G. O. Garcia, "Automatic induction machine parameters measurements using standstill frequency-domain tests", IET Electric Power Applications, Vol. 1, No. 5, 2007, pp. 833-838.

[8] L. A. S. Ribeiro, C. B. Jacobina, A. M. N. Lima, A. C. Oliveira, "Real-time estimation of the electric parameters of an induction machine using sinusoidal PWM voltage waveforms", IEEE Trans. Industry Appl., Vol. 36, No. 3, 2000. pp. 743-754.

[9] C. B. Jacobina, J. E. C. Filho, A. M. N. Lima, "Estimating the parameters of induction machine at standstill", IEEE Trans. Energy Conversion, Vol. 17, No.1, March 2002, pp. 85-89.

[10] S. Jafarzadeh, C. Lascu, S. Fadali, "State estimation of induction motor drives using the unscented Kalman filter", IEEE Trans. Industrial Electronics, Vol. 59, 2012, pp. 4207-4216.

[11] A. Lalami, R. Wamkeue, I. Kamwa, M. Saad, J. J. Beaudoin, "Unscented Kalman filter for non-linear estimation of induction machine parameters", IET Electric Power Applications, Vol. 6, No. 9, 2012, pp. 611-620.

[12] E. Laroche, E. Sedda, C. Durieu, "Methodological insights for online estimation of induction motor parameters", IEEE Trans. Control Syst. Technol., Vol. 16, No. 5, Sept. 2008, pp. 1021-1028.

[13] J. Stephan, M. Bodson, J. Chiasson, "Real-time estimation of the parameters and fluxes of induction motors", IEEE Trans. Industry Appl., Vol. 30, 1994, pp. 746-758.

[14] M. Cirrincione, M. Pucci, G. Cirrincione, G. A. Capolino, "A new experimental application of least-squares techniques for the estimation of the induction motor parameters" IEEE Trans. Industry Appl., Vol. 39, 2003, pp. 1247-1256.

[15] M. Cirrincione, M. Pucci, G. Cirrincione, G. A. Capolino, "Constrained minimization for parameters estimation of induction motor in saturated and unsaturated conditions" IEEE Trans. Industrial Electronics, Vol. 52, 2005, pp. 1391-1402.

[16] M. Cirrincione, M. Pucci, "Identification of an induction motor with the least-squares method", Elect. Eng. Res. Rep., No. 10, Dec. 2000, pp. 22-30.

[17] Kojooyan-Jafari, H., Monjo, Ll., Córcoles, F., Pedra, J.; ´Parameter estimation of wound-rotor induction motors from transient measurements, IEEE Trans. Energy Conversion, Vol. 29, No.2, 2014, pp. 300-308.

[18] S. R. Shaw, S. B. Leeb, "Identification of induction motor parameters from transient stator current measurements", IEEE Trans. Industrial Electronics, Vol. 46, 1999, pp. 139-149.

[19] R. Wamkeue, D. Aguglia, M. Lakehal, P. Viarouge, "Two-step method for identification of nonlinear model of induction machine", IEEE Trans. Energy Conversion, Vol. 22, No.4, Dec. 2007, pp. 801-809.

[20] J. A. de Kock, F. S. van der Merwe, H. J. Vermeulen, "Induction motor parameter estimation through an output error technique", IEEE Trans. Energy Conversion, Vol. 9, No.1, March 1994, pp. 69-76.

[21] R. Wamkeue, I. Kamwa, M. Chacha, "Unbalanced transients-based maximum likelihood identification of induction machine parameters", IEEE Trans. Energy Conversion, Vol. 18, No.1, March 2003, pp. 33-40.

[22] C. Grantham, D. J. McKinnon, "Rapid parameter determination for induction motor analysis and control", IEEE Trans. Industry Appl., Vol 39, No. 4, 2003, pp. 1014-1020.

[23] Whei-Min Lin, Tzu-Jung Su, Rong-Ching Wu, "Parameter identification of induction machine with a starting no-load low-voltage test", IEEE Trans. Industrial Electronics, Vol. 59, No. 1, Jan. 2012, pp. 352-360.

[24] J. Pedra, L. Candela, L. Sainz, "Modeling of squirrel-cage induction motors for electromagnetic transient", IET Electric Power Applications, Vol. 3, No. 2, March 2009, pp. 111-122.

[25] Ll. Monjo, F. Corcoles, J. Pedra, "Saturation effects on torque- and current-slip curves of squirrel-cage induction motors" IEEE Trans. Energy Conversion, Vol. 28, No. 1, 2013, pp. 243-254

[26] F. Corcoles, J. Pedra, M. Salichs, L. Sainz, "Analysis of the induction machine parameter identification" IEEE Trans. Energy Conversion, Vol. 17, No 2, June 2002, pp. 183-190.

[27] J. Pedra, F. Córcoles, "Estimation of induction motor double-cage model parameters from manufacturer data", IEEE Trans. Energy Conversion, Vol. 19, No 2, June 2004, pp. 310-317.

[28] J. Pedra, "On the determination of induction motor parameters from manufacturer data for electromagnetic transient programs" IEEE Trans. Power Systems, Vol. 23, No. 4, November 2008, pp. 1709-1718 .

[29] power_AsynchronousMachineParams. The Mathworks Inc.: MATLAB Release 2012a, available at http://www.mathworks.com.

[30] R. Babau, I. Boldea, T. J. E. Miller, N. Muntean, "Complete parameter identification of large induction machines from no-load acceleration-deceleration tests", IEEE Trans. Industrial Electronics, Vol. 54, No. 4, 2007, pp. 1962-1972.

[31] The MathWorks, Inc., *Matlab 7.9 (2009b)*. Natick, MA: 2009.